PURPOSE-LED
PUBLISHING™

PAPER

Audio and ultrasonic responses of laminated fluoroethylenepropylene and porous polytetrafluoroethylene films with different charge distributions

View the article online for updates and enhancements.

Audio and ultrasonic responses of laminated fluoroethylenepropylene and porous polytetrafluoroethylene films with different charge distributions

Xiaoqing Zhang[1,2]**, Gerhard M Sessler**[2]**, Yuan Xue**[1] **and Xingchen Ma**[1]

[1] Shanghai Key Laboratory of Special Artificial Microstructure Materials and Technology and School of Physics Science and Engineering, Tongji University, Siping Road 1239, Shanghai 200092, People's Republic of China
[2] Institute for Telecommunications Technology, Merckstrasse 25, 64283 Darmstadt, Germany

E-mail: g.sessler@nt.tu-darmstadt.de

CrossMark

Abstract

Laminated fluoropolymer films with a regular microstructure were made from compact fluoroethylenepropylene (FEP) and porous polytetrafluoroethylene (PTFE) using a process consisting of patterning and fusion bonding steps. The fabricated films were rendered piezoelectric via the contact charging or corona charging methods. The piezoelectric responses of such piezoelectret films were measured in the frequency range 100 Hz–100 kHz. The results show that the acoustic impedance of the FEP/PTFE films is around 0.014–0.030 MRayl. Dynamic piezoelectric d_{33} coefficients of up to 500 pC N^{-1} were achieved at 100 Hz for these films. Microphones built with such films exhibit flat response curves in a broad frequency range if the diffraction effects are eliminated. Bonded films with all positive charges deposited in the porous PTFE layers show the best thermal stability: after annealing for 1100 min at 125 °C, the remaining d_{33} at 1020 Hz is about 30% of the initial value, corresponding to 105 pC N^{-1}, and it remains relatively stable at this temperature. This remarkable thermal stability has to be attributed to the fact that positive charges are more permanent in porous PTFE than in FEP. The entire charge distribution exhibits much better thermal stability than is achievable for customary polypropylene piezoelectrets.

Keywords: piezoelectret, audio and ultrasonic responses, improved thermal stability, laminated FEP/porous PTFE, charge distribution

(Some figures may appear in colour only in the online journal)

1. Introduction

Piezoelectrets or ferroelectrets are charged polymer foams that exhibit a piezoelectric effect [1–4]. They were first described by scientists in Finland around 20 years ago [1]. The polarization of a piezoelectret is normally a bipolar space-charge, arranged to form oriented 'macroscopic dipoles' along the thickness of the film. Two essential features determine the working principle of piezoelectrets: the soft void structure in the polymer and the quasi-permanent positive and negative charges trapped in the polymer's matrix in a specific way [5–7]. These oriented macroscopic dipoles, together with the low Young's modulus of the polymer foam (normally of an order of magnitude of 0.1 to several MPa), result in large piezoelectric d_{33} coefficients, which are a factor of 20 higher than those of piezoelectric PVDF or its copolymers [2–4]. In addition, due to their very low bulk density (~330 kg m^{-3}), small sound velocity, and small relative permittivity (~1.5), piezoelectrets have very small acoustic impedance (~0.03 MRayl) and large piezoelectric g_{33} coefficients and figures of merit.
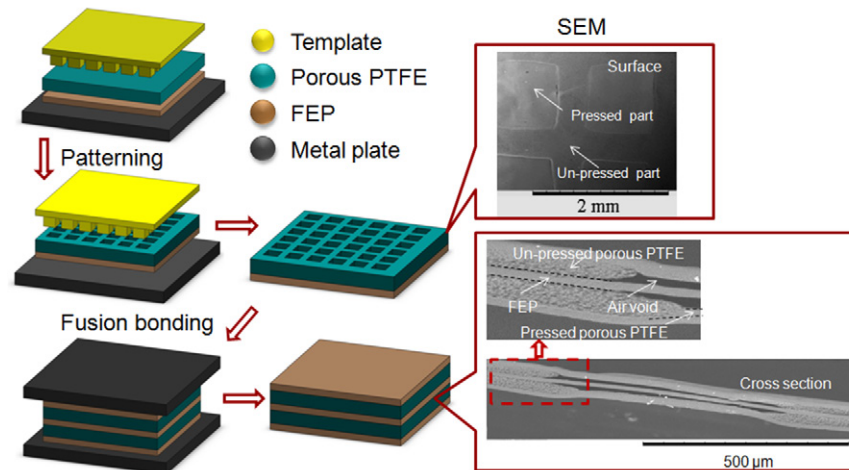
Figure 1. Fabrication process for the laminated FEP/PTFE films. Schematic of the fabrication process consisting of patterning the porous PTFE layer and fusion bonding the FEP and porous PTFE.

These new functional materials have received more attention from researchers and technology engineers because they can be used in many applications, such as acoustic transducers [8–10], airborne ultrasonic transducers [8, 10–16], flexible electronic devices [17], blood pressure pulse transducers [18], micro vibration energy harvesters [19–21], and so on.

To date, most piezoelectret applications have been based on cellular polypropylene (PP) piezoelectret films. However, the low working temperature (normally lower than 60 °C) of cellular PP piezoelectrets, which is associated with the relatively poor thermal stability of the positive and negative charges in PP, means that they cannot be used at elevated temperatures. Therefore, in recent years much effort has been made to enhance the thermal stability of piezoelectrets, for example through chemical modification [22] or polarization at elevated temperatures [23] for cellular PP films, and to develop new piezoelectrets based on thermally stable space-charge electret films. Among the newly implemented thermally stable piezoelectrets, the films made from fluorocarbon polymers, especially fluoroethylenepropylene (FEP) or/and polytetrafluoroethylene (PTFE), are very promising because FEP and PTFE are the most thermally stable polymer electret materials known so far.

In prior work, thermally stable piezoelectret films with artificially controlled void structures, made from FEP and porous PTFE layers, were prepared using patterning and fusion bonding methods [24–30]. Their thermal stability was tested by measuring the quasi-static piezoelectric d_{33} coefficients of samples annealed at elevated temperatures. The results showed that laminated FEP/patterned porous PTFE films, referred to here as FEP/PTFE films, exhibit the best thermal stability if all positive charges are deposited in the porous PTFE layer [26, 27]. Other studies indicate that the piezoelectric d_{33} coefficients determined using different methods, such as the quasi-static, dielectric spectrum, and acoustic techniques, are sometimes very different [27, 28, 30]. This is due to the different excitation mechanisms of the samples, namely mechanical force, rf field, or acoustic wave, applied to either the surface or the volume of the sample. Among these measuring

methods, the acoustic method is a good choice because it not only gives an average value of d_{33} over the whole sample area in a broad frequency range, but also yields reliable values even if the surface of the samples is not flat [28].

Based on our prior work [26, 27], this study includes laminated FEP/PTFE piezoelectret films with different annealing treatments and utilizes measurements in the acoustic and ultrasonic frequency ranges. In addition, the thermal stability of d_{33} in FEP/PTFE films with different charge distributions is further analyzed via measurements of the surface potential decay.

2. Details of experiments

2.1. Preparation of FEP/PTFE piezoelectret films

A similar but improved preparation process to that reported in the literature was used for the fabrication of the laminated FEP/PTFE films [26]. Again, rigid templates with a periodic square-array surface structure were utilized to generate regular profile patterns in the porous PTFE layers. Three types of templates with different dimensional parameters (as shown in the inset of figure 5, below) were used. The polymer films employed were 12.5 μm thick FEP and 25 μm thick porous PTFE (porosity > 90%), and these were provided by DuPont. The preparation process, shown schematically in figure 1, mainly consisted of patterning the porous PTFE layers and then fusion bonding the FEP and patterned porous PTFE layers [26]. In more detail, the FEP and porous PTFE layers were cut into small pieces with an area of 5 cm × 5 cm. In the patterning step, a stainless steel plate with a very smooth surface was used to support the films. An FEP layer was put onto the mirror side of the metal plate and then a porous PTFE layer was placed onto it. Thereafter, a template with its patterned surface facing the porous PTFE layer was placed on top of the porous PTFE layer. Then, the stacks were pressed using a Platen Vulcanizing Press machine at room temperature and a pressure of 3 MPa for ~4 min. This resulted in a patterned porous PTFE layer on an FEP layer and finished the

patterning step. The upper SEM image in figure 1 shows a top view of the patterned layers obtained after the patterning step.

In the following fusion bonding step, two patterned layers and one FEP layer were stacked together and then sandwiched between a pair of glass plates. Finally, they were put into an oven with a temperature of 280 °C for fusion bonding between the FEP and porous PTFE layers. The completed samples consisted of three compact FEP layers and two patterned porous PTFE layers. An SEM image of a cross-section of a fabricated film is also shown in figure 1.

To build up oriented 'macroscopic dipoles' in the laminated FEP/PTFE films and thus render them piezoelectric (piezoelectrets), both contact charging and corona charging methods were used. For the contact charging, the samples were first metalized on both sides with Al electrodes. A triangular-shaped voltage pulse of 20 ms duration with peak amplitudes between 500–3500 V, supplied from a Radiant Precision Workstation Materials Analyzer, was applied to the sample. The resulting charges on the electrodes were measured during voltage application and an electric hysteresis loop was obtained, indicating the build-up of 'macroscopic dipoles' in the inner voids.

Depending on the arrangement of the layers, three different kinds of samples were obtained, denominated I, II, and III in figure 2. One can also obtain the samples with different charge distributions, as shown in figure 2, using corona charging. However, in order to investigate charge stability in laminated FEP/PTFE films, some samples were made by fusion bonding a *single* FEP-patterned porous PTFE layer, as shown schematically in section 3.4. Such samples were charged using a grid-voltage controlled corona charging setup. All the samples were charged at room temperature.

2.2. Measurement of acoustic impedance

The acoustic impedance Z of the laminated FEP/PTFE piezoelectret films can be obtained from the relation $Z = \rho v$, where ρ is the density of the material and v is the velocity of sound in the medium. The velocity v can be calculated using the relation $v = 2N_t$ by measuring the thickness mode frequency constant N_t of the material [31]. In this study, we measured the dielectric resonance spectrum of the laminated FEP/PTFE samples using a high impedance analyzer (Agilent 4294A), after which the resonance frequency f_r could be read directly from the dielectric resonance spectra. Once the resonance frequency f_r is found, the frequency constant N_t can also be determined by $N_t = f_r t$, where t is the thickness of the sample. This thickness was measured using a thickness gauge (type F-55) with an applied pressure of 0.36 kPa in this study. The density of the samples was determined by weighing and measuring their volume.

2.3. Measurement of acoustic and ultrasonic responses

The setup described in the literature [32] was utilized for the measurement of the acoustic and ultrasonic responses of the laminated FEP/PTFE films. In this study, the laminated FEP/PTFE piezoelectet samples had a circular shape and an area of 3.14 cm². The samples were covered with 100 nm
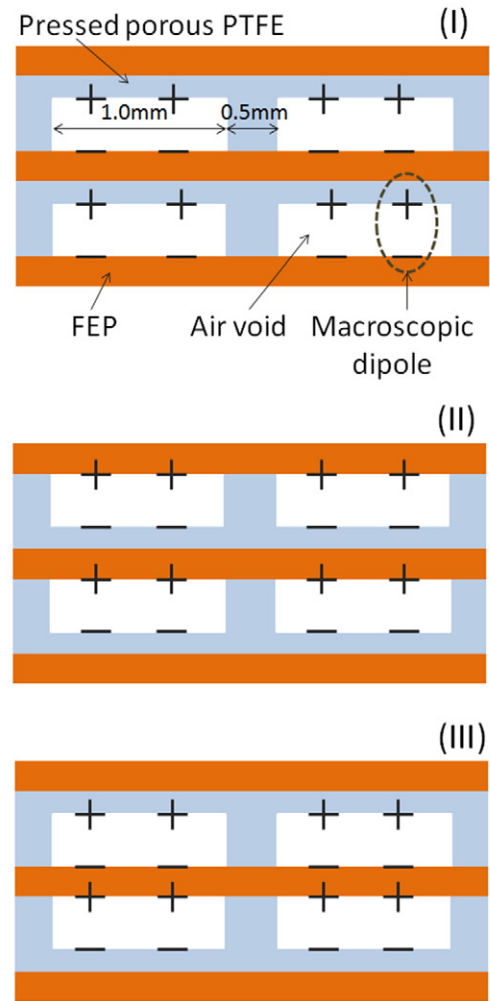

Figure 2. Schematic views of the microstructure and charge distribution in laminated FEP/PTFE piezoelectret films. Type I: all the positive charges are deposited on the compressed porous PTFE layer, while all the negative charges are placed on the FEP layer. Type II: the situation is reversed, i.e. the negative and positive charges are trapped in the FEP and compressed porous PTFE layers, respectively. Type III: the film has a symmetrical microstructure, and the positive and negative charges are trapped in either the FEP or the compressed porous PTFE.

thick Al electrodes on both surfaces, and glued onto a provisional microphone case using double-sided adhesive conductive tape. An active dynamic loudspeaker with a broadband response from 1–100 kHz, controlled by an audio analyzer (Rhode & Schwarz Audio Analyzer UPD), was utilized as sound source. The loudspeaker and the piezoelectret microphone were set in an anechoic chamber (B&K Anechoic Test Chamber, type 4222). The distance between the loudspeaker and the piezoelectret microphone was 15 cm. The output voltage V generated by the microphone as excited by the loudspeaker was recorded using the same audio analyzer. A calibrated free-field 1/4″ condenser microphone (B&K 4135) was used to determine the reference free-field sound pressure p_{ff} at the location of the piezoelectret microphone using a replacement method. Therefore, the free-field sensitivity M_{ff} of the piezoelectret microphone is given by $M_{ff} = V/p_{ff}$.

To calculate the dynamic piezoelectric d_{33} coefficient from the microphone sensitivity, the pressure sensitivity of the piezoelectret microphones is required. This sensitivity is defined as $M_p = V/p$, where p is the actual sound pressure p in front of the microphone after it is positioned in the sound field. This sound pressure differs from the free-field value p_{ff} at higher frequencies because of diffraction effects [29]. The value of p was determined from p_{ff} by means of the free-field correction factor [33]. From such evaluations M_p was obtained [29] and the dynamic piezoelectric d_{33} coefficient of the piezoelectret was obtained by means of [28]

$$d_{33} = M_p \cdot C_F/A_F, \tag{1}$$

where C_F is the capacitance and A_F is the area of the piezoelectret sample.

In this study, we also used a charge amplifier (B&K 2635) to record the charges flowing, in response to an incident sound wave, between the short-circuited electrodes of the microphones. Similar equipment to the above was used to generate the sound field and determine the free-field sound pressure level p_{ff}. To obtain the voltage sensitivity M_{ff} from the charge response, the relation $V = \sigma_i/C$, where σ_i is the induced charge density on the electrode and C is the sample capacitance, was used and $M_{ff} = \sigma_i/C \, p_{ff}$ was calculated. In addition, the dynamic piezoelectric d_{33} coefficients can be determined by $d_{33} = \sigma_i/p$. Again, the value p was determined from P_{ff} by means of the free-field correction factor [33].

2.4. Measurements of isothermal decay

For valuation of the thermal stability of the piezoelectric effect in the laminated FEP/PTFE films, the samples were annealed at an elevated temperature of 125 °C and the dynamic d_{33} coefficients were measured at room temperature using the acoustic method mentioned above.

In the study of the thermal stability of charges in the laminated FEP/PTFE films the samples were annealed at the same elevated temperature for a definite amount of time before the surface potentials were measured at room temperature using a compensation method (Trek Model 370).

3. Results and discussion

3.1. Charge density after contact charging

Figure 3 shows the electrode charge density σ_i as a function of the applied ac-bias voltage, indicating the corresponding electric hysteresis loops and the relationship between the quasi-permanent charge density on the electrodes and the maximum ac-bias voltage for a laminated film. Figure 3(a) illustrates that a very thin electric hysteresis loop can be recorded when an ac-bias voltage with a peak value of ± 1500 V is applied to the sample, indicating an onset of dielectric barrier discharge (DBD) in the inner voids. With increasing ac-bias voltage, the electric-hysteresis loops become more prominent, leading to an enhancement of the quasi-permanent charge density on the electrodes after removal of the ac-voltage, as shown in figures 3(b). The quasi-permanent charge density σ_i on the
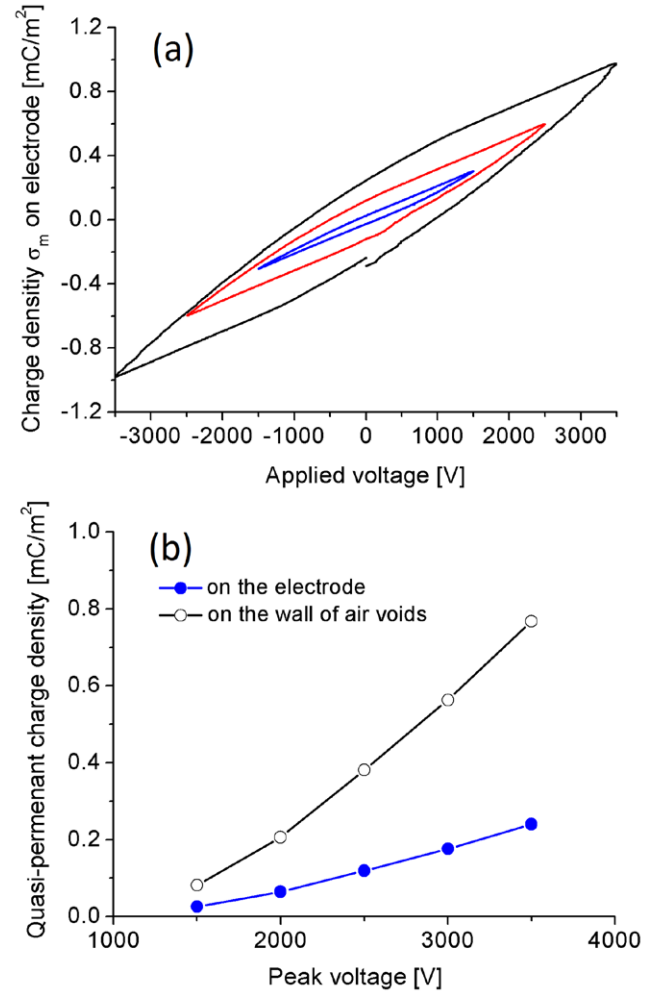

Figure 3. Electric hysteresis loop (a) and quasi-permanent charge density σ_0 on inner voids and induced charge density σ_i on the electrodes after removal of the applied voltage (b).

electrodes reaches 0.24 mC m^{-2} at an applied ac-bias voltage of ± 3500 V. The charge densities σ_0 on the inner walls of the voids, also shown in figure 3(b), are discussed below.

Larger bias voltages would be required to achieve saturation of the charge density in the hysteresis loops of figure 3(a), which would be a clear indication of ferroelectric properties [2, 34]. Unfortunately, such high voltages would destroy the samples. However, strong evidence of ferroelectric behavior is provided by the butterfly shape of the electromechanical strain curves found in other experiments [2, 35]. This distinguishes the ferroelectric responses from purely resistive, non-ferroelectric loops [34].

In order to evaluate the possible contributions of charge injection and interfacial polarization between the electrodes and the polymer surfaces to the quasi-permanent trapping of charge, a reference experiment was performed. In this investigation, an electric field of 80 MV m^{-1} was applied to the laminated FEP/PTFE film, generating an electric field of 80 MV m^{-1} in the sample, which is much higher than the field of 20 MV m^{-1} due to the maximum ac-bias voltage of ± 3500 V. A quasi-permanent charge density of less than 0.01 mC m^{-2} was observed. Therefore, under the given experimental
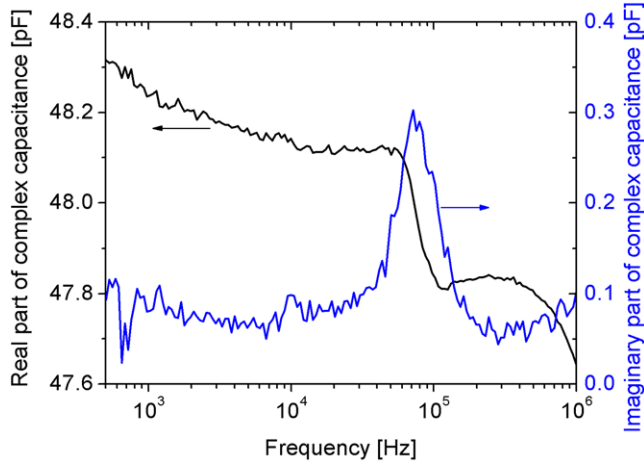
Figure 4. Dielectric resonance spectrum for a laminated FEP/PTFE piezoelectret film.

conditions, the effects of possible charge injection and interfacial polarization between electrodes and polymer surfaces are negligible, and the breakdown in the air voids is the dominant charging mechanism.

The charge density σ_0 on the walls of the inner voids, also shown in figure 3(b), may be calculated from the charge densities σ_i on the electrodes by taking into account the geometry of the voids and the thickness of the air and solid layers [29]. The sample shown in figure 3 consists of three layers of FEP and two layers of patterned porous PTFE, and the patterning ratio α, defined as the ratio of the area covered by the air voids to the total sample area, is 44%. For the calculations we assume that the charge density on the walls of the inner voids is uniform and has the same magnitude σ_0 everywhere. Then the relation between the induced charge densities σ_i and σ_0 is given by [29]

$$\sigma_i = \frac{\alpha \varepsilon_r \sum_i s_{2i} \sigma_0}{s_1 + \varepsilon_r s_2}, \qquad (2)$$

where ε_r is the relative permittivity of the solid layer, s_{2i} is the thickness of the ith air void, s_1 is the total thickness of the solid layers, and s_2 is the total thickness of the air voids. The pressed part of the patterned porous PTFE has a thickness of 2.5 μm and the same relative permittivity as FEP (2.3), and the values of s_{2i}, s_1, and s_2 are 22.5, 42.5, and 45 μm in this sample, respectively. Taking these values, together with $i = 2$, $\sigma_i = 0.24$ mC m^{-2}, and $\alpha = 44\%$, one obtains from equation (2) $\sigma_0 = 0.77$ mC m^{-2}. The calculated charge densities on the walls of the inner voids are also shown in figure 3(b). Internal charge densities have previously been calculated for other kinds of piezoelectrets too. Thus, for the frequently used PP piezoelectrets charge densities from about 0.4 to 0.9 mC m^{-2} have been determined [36, 37], while for patterned FEP piezoelectrets the calculated values are approximately 0.5 mC m^{-2} [29].

3.2. Acoustic impedance

The complex capacitance spectrum near the resonance and anti-resonance frequencies for a laminated FEP/PTFE film

sample, in a free boundary condition, is shown in figure 4. The sample has an area of 3.14 cm^2, a thickness of 100 μm, and a measured bulk density of 1.19×10^3 kg m^{-3}. Figure 4 indicates that the resonance frequency, corresponding to the thickness extension, appears at about 60 kHz, which indicates that the acoustic impedance of the laminated film is about 0.014 MRayl. Our experimental data show that the acoustic impedance for a normal PP piezoelectret film (expanded PQ50 PP film) with a bulk density of 403 kg m^{-3} and a thickness of 77 μm is about 0.025 MRayl. Therefore, the value of the acoustic impedance in the tested laminated FEP/PTFE film is slightly smaller than that of normal PP piezoelectret films and much smaller than that of PVDF (~2.4 MRayl), suggesting that laminated FEP/PTFE piezoelectret films are promising materials for airborne ultrasonic transducers. Experimental results on the dielectric resonance spectra for the laminated FEP/PTFE samples show that the typical value of the relative permittivity in such films is around 1.7. The acoustic impedance and relative permittivity in laminated FEP/PTFE piezoelectret films are associated with the thickness and density of the films, which can be tuned by controlling the parameters of the preparation process. Our experimental results indicate that the acoustic impedance varies in the range of 0.014–0.030 MRayl as the thickness of the films changes in the range of 100–70 μm.

The dielectric resonance spectrum can also be used to determine Young's modulus Y_3 of the piezoelectret films in the thickness direction [38, 39]. Once the anti-resonance frequency f_a is read from the dielectric spectrum, Young's modulus Y_3 is given by

$$Y_3 = 4f_a^2 t^2 \rho. \qquad (3)$$

For the tested sample in figure 4, the anti-resonance frequency is about 73 kHz. Taking the thickness of 100 μm and the bulk density of 1.19×10^3 kg m^{-3}, one obtains $Y_3 = 0.25$ MPa from equation (3).

3.3. Acoustic and ultrasonic responses

For the investigation of the acoustic and ultrasonic responses of the laminated FEP/PTFE films, microphones were built up with the films and their free-field sensitivities M_{ff} were measured using the setup and method mentioned in section 2.3. Figure 5 shows the results for the responses of four samples, based on four types of laminated films with different microstructure parameters (a and b, explained in the inset of the figure) and patterning ratios α, explained in section 3.1. This figure indicates that all the tested samples show very similar behavior in the experimental frequency range.

Below 1 kHz, the responses decrease slightly with increasing frequency. This is due to the fact that the microphone sensitivities are inversely proportional to Young's modulus [40], which increases slightly with frequency. This increase was found for many polymers, including solid FEP, PTFE, and PP, in the frequency range from about 10^2–10^6 Hz [41], and previous measurements in the authors' laboratory also confirmed it for cellular PP [42].
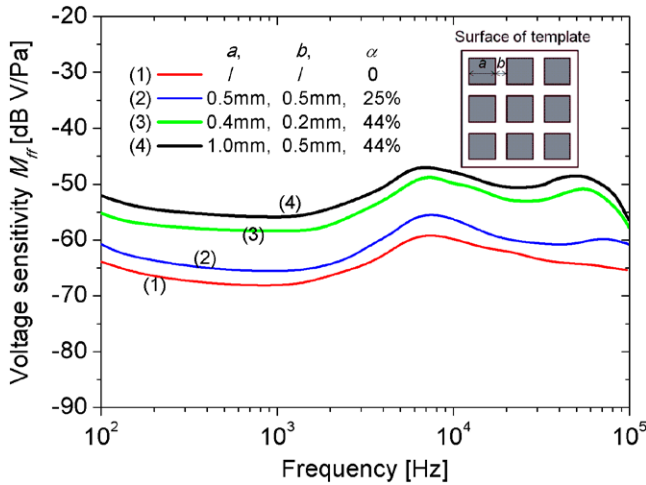
J. Phys. D: Appl. Phys. 49 (2016) 205502

X Zhang *et al*

Figure 5. Frequency responses of the free-field voltage sensitivity for the laminated FEP/PTFE films with different microstructure parameters. α is the ratio of the area covered by the air voids to the total sample area.

Figure 6. Dynamic piezoelectric d_{33} coefficient determined by acoustic measurements (see figure 5) for a laminated FEP/PTFE piezoelectret film.

Above 1 kHz the responses increase significantly and reach a peak at about 10 kHz. This can be explained by the diffraction effects at the microphone housing when the housing dimensions are comparable to the wavelength of the sound [28, 32, 37]. The peaks at about 50 kHz are probably associated with the thickness resonance of the films [32].

Figure 5 also indicates that the patterning ratio α affects the response of the films significantly: the response can be enhanced by increasing α. The sample with a patterning ratio α of 0 (i.e. the film has been fabricated with FEP and un-patterned porous PTFE layers) has a response of about -68 dB (ref. 1 V Pa^{-1}) at 1 kHz, while the response for the sample with α of 44% can reach up to -56 dB. This could be due to the increase of the charging capability and the reduction of Young's modulus with the increase of α [26, 27]. Compared with the tiny air gaps formed by the fibers in porous PTFE, the air in the large voids formed by the patterned porous PTFE and compact FEP is more easily ionized during charging under the present experimental conditions, leading to relatively large charge density. On the other hand, with the increase of α, more large voids are formed in the laminated films, resulting in a decrease of Young's modulus in the films. This was confirmed by Young's modulus values determined from the dielectric resonance spectra [27].

According to the accepted model for piezoelectrets, the piezoelectric d_{33} coefficient is proportional to the charge density σ_0 on the inner voids, but inversely proportional to Young's modulus. Therefore, both the enhancement of the charge density and the reduction of Young's modulus in the laminated films with larger α contribute to the increase of the response. The results for samples (3) and (4) in figure 5 indicate that the size of the voids (determined by the template parameter a in this study) is another factor that affects the response of the films. Even for films with the same α, the response can be further improved by increasing the size of the voids. More work will be done to further understand the relation between the piezoelectric effect and the parameters of the microstructure in the laminated films.
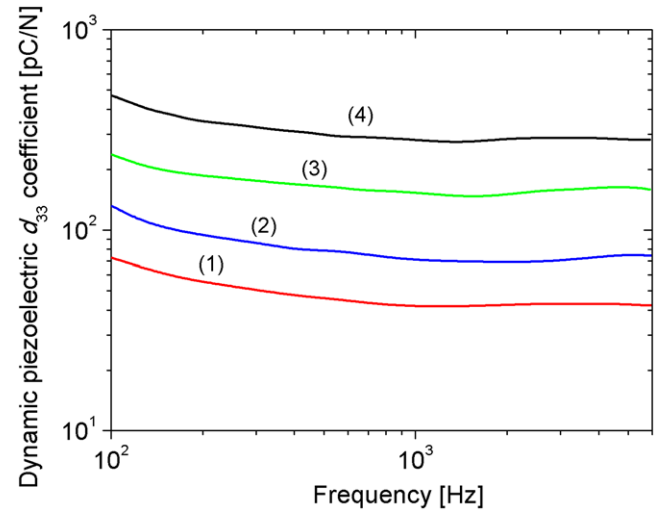
The results shown in figure 5 allow one to determine the dynamic piezoelectric d_{33} coefficients from the microphone sensitivity by first converting M_{ff} into the pressure sensitivity M_{p} and then using equation (1). The sensitivity conversion is performed by considering the diffraction effects [32, 33], taking the frontal area of the entire microphone into account, including its mounting. In this study, the frontal area is 9.62 cm^2. The results for the dynamic d_{33} coefficients for the frequency range 100 Hz–6 kHz obtained from the microphone data in figure 5 are shown in figure 6. Again, the frequency response of d_{33} decreases slightly with increasing frequency for the reason mentioned above. A dynamic d_{33} coefficient of around 500 pC N^{-1} is achieved at 100 Hz, while a quasi-static d_{33} coefficient of 307 pC N^{-1} is measured for the same tested sample in figures 5 and 6. Compared with the quasi-static d_{33} coefficients, normally larger dynamic d_{33} values are obtained when using the acoustic method for the samples with $\alpha \neq 0$. This is in agreement with the relevant results reported in the literature [27], where the dynamic d_{33} coefficient determined via the dielectric resonance spectra is larger than the values obtained in the quasi-static measurement. This is explained by the non-flat surfaces of the films with $\alpha \neq 0$, where some of the voids are deformed during the evaporation of the metal electrodes. Therefore, in the quasi-static measurement, only part of the sample can be excited, while the acoustic measurements give an average d_{33} value over the whole sample [28]. The experimental results obtained in this study thus further verify the explanation in the literature.

3.4. Thermal stability of FEP/PTFE film

Since both charge polarities are involved in piezoelectrets, the thermal stabilities of the positive and negative charges on the walls of the inner voids are equally important for the thermal stability of the d_{33} coefficients. Although FEP and PTFE have the highest thermal charge stability of the polymers that we know of to date, the positive charges are normally less stable than the negative ones in these materials. This limits further
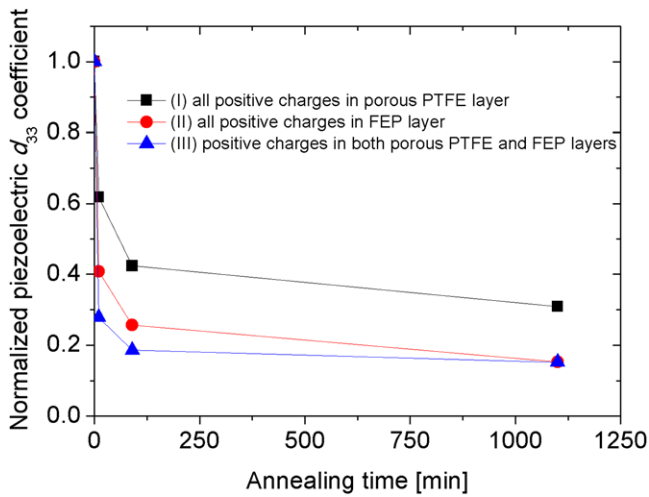
J. Phys. D: Appl. Phys. **49** (2016) 205502

X Zhang *et al*

Figure 7. Normalized piezoelectric d_{33} coefficient as a function of annealing time. The data were measured at 1020 Hz. The annealing temperature was 125 °C. The initial piezoelectric d_{33} coefficients for the tested samples of types I, II, and III were 340, 500, and 205 pC N^{-1}, respectively.

Figure 8. Isothermal decay of positive and negative charges trapped in FEP and porous PTFE layers at 125 °C.

improvement of the thermal stability in piezoelectrets based on these polymers. However, relevant research has indicated that the positive charges are thermally more stable in porous PTFE [43]. Therefore, it is of interest to design a microstructure and control the charge distribution in the piezoelectrets such that the thermal stability of the d_{33} coefficients is further improved. The piezoelectret preparation and corona charging process described in this paper makes it possible to design a cellular film that consists of air voids with porous PTFE walls and control the charge distribution in it. Figure 2 shows the three types of laminated FEP/PTFE films used in this study. In type I, all the positive charges are deposited on the compressed porous PTFE layer, while all the negative charges are placed on the FEP layer. In type II, the situation is reversed, i.e. the negative and positive charges are trapped in the compressed porous PTFE and FEP layers, respectively. In type III, the film has a symmetrical microstructure, and the positive and negative charges are trapped in both the FEP and compressed porous PTFE layers.

The results for the isothermal decay of the piezoelectric d_{33} coefficients at an annealing temperature of 125 °C for the film samples with different charge distributions are shown in figure 7. The data were obtained at 1020 Hz using the acoustic method. This figure illustrates that the film with all the positive charges trapped in the patterned porous PTFE layers (type I) exhibits the best thermal stability among the tested samples: after annealing at 125 °C for 1100 min, the remaining d_{33} is about 30% of the initial value, corresponding to 105 pC N^{-1}. Film types II and III have comparable thermal stability, but are less thermally stable than type I: after the same annealing time as sample type I, the d_{33} coefficients drop to about 20% of the initial values. These results confirmed the older results, which indicated that the thermal stability of the positive charges is better in porous PTFE than in compact FEP [43].

In order to observe the thermal stability of the charges in the films directly, isothermal decays of the surface potentials for positively and negatively charged single FEP and
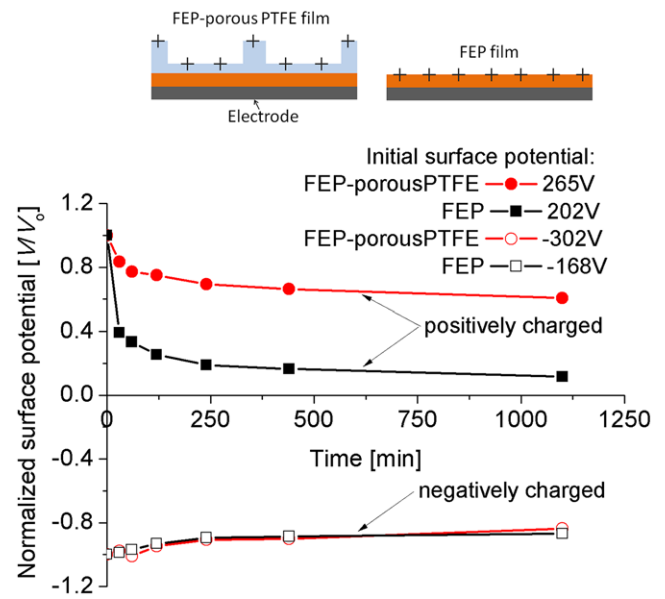
laminated FEP/PTFE films were measured. Figure 8 shows schematic views of the structures of the tested samples and the experimental results. Again, the samples were annealed at 125 °C. To obtain comparable charge densities on the surfaces of the tested samples, the thickness of the samples was taken into account when the grid voltages for controlling the initial surface potential were selected. The initial surface potentials obtained after corona charging for the four samples are also shown in figure 8. This figure indicates that the thermal stabilities of the *negative* charges trapped in the FEP and patterned porous PTFE layers are comparable. However, the difference for the *positive* charges is significant. The positive charges trapped in the patterned porous PTFE layer are much more thermally stable than those in the FEP layer. After an annealing time of 1080 min, the remaining surface potential of the positively charged FEP/PTFE film is about 61% of the initial value, while under the same conditions, the surface potential of the positively charged single FEP film decreases to about 12% of the initial value. These results agree qualitatively with the isothermal decay measurements for the d_{33} coefficients shown in figure 7. Therefore, the thermal stability can be further improved in fluoropolymer piezoelectrets by designing the microstructure and controlling the charge distribution.

4. Conclusions

Laminated FEP/PTFE piezoelectret films with different microstructures and charge distributions were prepared using a template-based process followed by corona charging. The results showed that the acoustic impedance of the FEP/PTFE films is around 0.014 MRayl. Dynamic piezoelectric d_{33} coefficients of up to 500 pC N^{-1} were achieved at 100 Hz in the FEP/PTFE films. Microphones built with such films exhibited relatively flat response curves in a broad frequency range if diffraction effects are eliminated. The films

with all the positive charges deposited in the porous PTFE layers showed the best thermal stability: after annealing at 125 °C for 1100 min, the remaining d_{33} at 1020 Hz was around 30% of the initial value, corresponding to about 105 pC N^{-1}, and was relatively stable at this temperature. This remarkably good thermal stability has to be attributed to the fact that positive charges are more permanent in porous PTFE than in FEP. The charges of both polarities, and thus the piezoelectric d_{33} coefficients, are much more stable than in PP.

Acknowledgments

References

[1] Lekkala J *et al* 1996 *Med. Biol. Eng. Comput.* **34** 67
[2] Bauer S, Gerhard-Multhaupt R and Sessler G M 2004 *Phys. Today* **57** 37
[3] Gerhard-Multhaupt R 2002 *IEEE Trans. Dielectr. Electr. Insul.* **9** 850
[4] Bauer S 2006 *IEEE Trans. Dielectr. Electr. Insul.* **13** 953
[5] Sessler G M and Hillenbrand J 1999 *Appl. Phys. Lett.* **75** 3405
[6] Paajanen M, Lekkala J and Kirjavainen K 2000 *Sensors Actuators* A **84** 95
[7] Mellinger A, Wegener M, Wirges W, Mallepally R and Gerhard-Multhaupt R 2006 *Ferroelectrics* **331** 189
[8] Kressmann R 2001 *J. Acoust. Soc. Am.* **109** 1412
[9] Hillenbrand J and Sessler G M 2004 *J. Acoust. Soc. Am.* **116** 3267
[10] Hillenbrand J and Sessler G M 2014 *Ferroelectrics* **472** 77
[11] Ealo J L, Camacho J J and Fritsch C 2009 *IEEE Trans. Ultrason. Ferroelctr. Freq. Control* **56** 848
[12] Strobel J, Rupitsch S J and Lerch R 2009 *IEEE Int. Ultrasonics Symp. Proc.* pp 398–401
[13] Jiméneza A, Hernándeza Á, Ureñaa J, Péreza M C, Álvarezb F J, Marzianic C D, Garcíaa J J and Villadangosa J M 2008 *Sensors Actuators* A **148** 342
[14] Rupitsch S J, Lerch R, Strobel J and Streicher A 2011 *IEEE Trans. Dielectr. Electr. Insul.* **18** 69
[15] Ealo J L, Seco F and Jimenez A R 2008 *IEEE Trans. Ultrason. Ferroelctr. Freq. Control* **55** 915
[16] Ealo J L, Prieto J C and Seco F 2011 *IEEE Trans. Ultrason. Ferroelctr. Freq. Control* **58** 1651
[17] Graz I, Kaltenbrunner M, Keplinger C, Schwödiauer R, Bauer S, Lacour S P and Wagner S 2006 *Appl. Phys. Lett.* **89** 073501
[18] Sorvoja H, Kokko V, Myllylä R and Miettinen J 2005 *IEEE Trans. Instrum. Meas.* **54** 2505
[19] Pondrom P, Hillenbrand J, Sessler G M, Bös J and Melz T 2014 *Appl. Phys. Lett.* **104** 172901
[20] Anton S R, Farinholt K M and Erturk A 2014 *J. Intell. Mater. Syst. Struct.* **25** 1681
[21] Zhang X, Wu L and Sessler G M 2015 *AIP Adv.* **5** 077185
[22] An Z, Zhao M, Yao J, Zhang Y and Xia Z 2009 *J. Phys. D: Appl. Phys.* **42** 015418
[23] Zhang J-W, Lebrun L, Guiffard B, Belouadah R, Guyomar D, Garbuio L, Cottinet P-J and Liu Q 2011 *J. Phys. D: Appl. Phys.* **44** 415403
[24] Altafim R A C, Basso H C, Gongalves Neto L, Lima L, Altafim R A P and de Aquino C V 2005 *IEEE Conf. on Electrical Insulation and Dielectric Phenomena* (Piscataway, NJ: IEEE Service Center) pp 669–72
[25] Altafim R A P, Qiu X, Wirges W, Gerhard R, Altafim R A C, Basso H C, Jenninger W and Wagner J 2009 *J. Appl. Phys.* **106** 014106
[26] Zhang X, Cao G, Sun Z and Xia Z 2010 *J. Appl. Phys.* **108** 064113
[27] Lou K, Zhang X and Xia Z 2012 *Appl. Phys.* A **107** 613
[28] Zhang X, Hillenbrand J and Sessler G M 2007 *J. Appl. Phys.* **101** 054114
[29] Zhang X, Hillenbrand J, Sessler G M, Haberzettl S and Lou K 2012 *Appl. Phys.* A **107** 621
[30] Gerard M, Bowen C R and Osman F H 2011 *Ferroelectrics* **422** 59
[31] Rosen C Z, Hiremath B V and Newnham R 1991 *Piezoelectricity* (New York: American Institute of Physics)
[32] Zhang X, Zhang X W, Sessler G M and Gong X 2014 *J. Phys. D: Appl. Phys.* **47** 015501
[33] Rasmussen G 1980 *J. Acoust. Soc. Am.* **68** 70
[34] Scott J F 2008 *J. Phys.: Condens. Matter* **20** 021001
[35] Lindner M, Hoislbauer H, Schwödiauer R, Bauer-Gogonea S and Bauer S 2004 *IEEE Trans. Dielectr. Electr. Insul.* **11** 255
[36] Paajanen M, Välimäki H and Lekkala J 2000 *J. Electrost.* **48** 193
[37] Hillenbrand J, Sessler G M and Zhang X 2005 *J. Appl. Phys.* **98** 064105
[38] Neugschwandtner G S, Schwödiauer R, Vieytes M, Bauer-Gogonea S, Bauer S, Hillenbrand J, Kressmann R, Sessler G M, Paajanen M and Lekkala J 2000 *Appl. Phys. Lett.* **77** 3827
[39] Mellinger A 2003 *IEEE Trans. Dielectr. Electr. Insul.* **10** 842
[40] Hillenbrand J and Sessler G M 2000 *IEEE Trans. Dielectr. Electr. Insul.* **7** 537
[41] Lagakos N, Jarzynski J, Cole J H and Bucaro J A 1986 *J. Appl. Phys.* **59** 4017
[42] Hillenbrand J, Zhang X, Zhang Y and Sessler G M 2003 *2003 Annual Report, IEEE Conf. on Electrical Insulation and Dielectric Phenomena* pp 40–3
[43] Xia Z, Gerhard-Multhaupt R, Künstler W, Wedel A and Danz R 1999 *J. Phys. D: Appl. Phys.* **32** L83